Science Advances
AAAS

Supplementary Materials for

Lachnospiraceae-derived butyrate mediates protection of high fermentable fiber against placental inflammation in gestational diabetes mellitus

Shuangbo Huang *et al.*

Corresponding author: Chengquan Tan, tanchengquan@scau.edu.cn

Sci. Adv. **9**, eadi7337 (2023)
DOI: 10.1126/sciadv.adi7337

This PDF file includes:

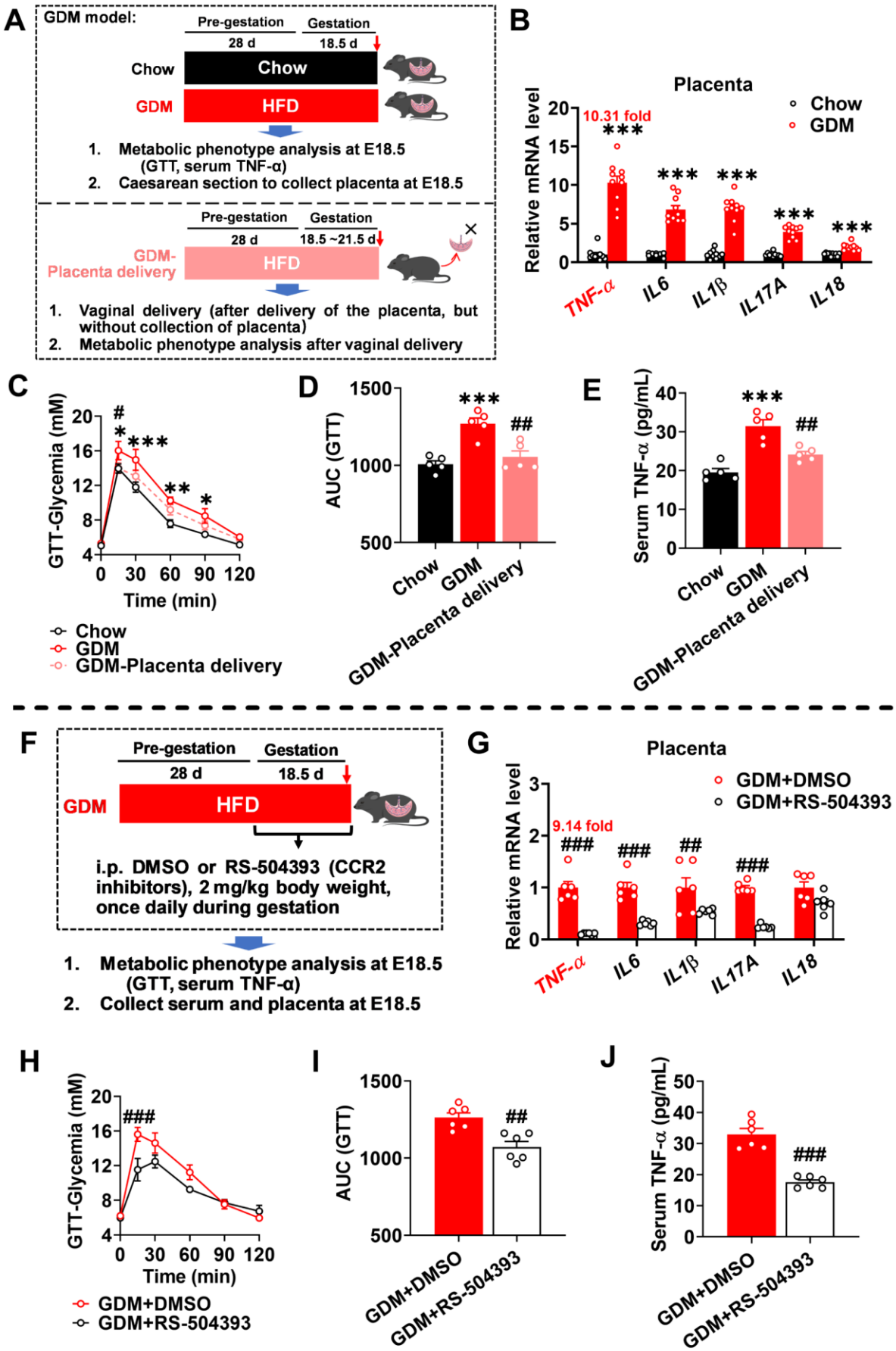
A
GDM model:
Pre-gestation
Gestation
28 d
18.5 d
Chow
Chow
GDM
HFD
1. Metabolic phenotype analysis at E18.5 (GTT, serum TNF-α)
2. Caesarean section to collect placenta at E18.5
Pre-gestation
Gestation
28 d
18.5 ~21.5 d
GDM-Placenta delivery
HFD
1. Vaginal delivery (after delivery of the placenta, but without collection of placenta)
2. Metabolic phenotype analysis after vaginal delivery
B
Placenta
Chow
GDM
Relative mRNA level
10.31 fold
TNF-α
IL6
IL1β
IL17A
IL18
C
GTT-Glycemia (mM)
Time (min)
Chow
GDM
GDM-Placenta delivery
D
AUC (GTT)
Chow
GDM
GDM-Placenta delivery
E
Serum TNF-α (pg/mL)
Chow
GDM
GDM-Placenta delivery
F
Pre-gestation
Gestation
28 d
18.5 d
GDM
HFD
i.p. DMSO or RS-504393 (CCR2 inhibitors), 2 mg/kg body weight, once daily during gestation
1. Metabolic phenotype analysis at E18.5 (GTT, serum TNF-α)
2. Collect serum and placenta at E18.5
G
Placenta
GDM+DMSO
GDM+RS-504393
Relative mRNA level
9.14 fold
TNF-α
IL6
IL1β
IL17A
IL18
H
GTT-Glycemia (mM)
Time (min)
GDM+DMSO
GDM+RS-504393
I
AUC (GTT)
GDM+DMSO
GDM+RS-504393
J
Serum TNF-α (pg/mL)
GDM+DMSO
GDM+RS-504393

Fig. S1. A model of GDM induced by HFD before and during pregnancy accompanied by placental inflammation. (**A**) Schematic of GDM induced by HFD before and during pregnancy (n = 5-6 mice/group). Eight-week-old female mice were fed standard chow diet (Chow) or HFD (GDM) during pre-gestation (prior to mating, 28 days) and post-gestation (E0.5 to E18.5, 18 days). (**B** and **G**) The mRNA levels of placental inflammatory factors at E18.5 (n = 10-12 placentae from 5-6 litters per group). (**C, D, H,** and **I)** GTT and AUC (n = 5-6 mice/group). **(E** and **J)** Serum TNF-α levels (n = 5-6 mice/group). **(F)** Schematic of the pharmacological blockade of CCL2/CCR2. HFD-fed mice were intraperitoneally injected with 2 mg/kg body weight RS-504393 or DMSO once daily during gestation. Data were analyzed by unpaired Student's t-test (B, G, I, and J), two-way ANOVA followed by post hoc Bonferroni tests (C and H) or one-way ANOVA followed by post hoc Tukey's tests (D and E), and represented mean ± SEM. **P* < 0.05, ***P* < 0.01, ****P* < 0.001, relative to the Chow group. #*P* < 0.05, ##*P* < 0.01, relative to the GDM or GDM+DMSO groups.

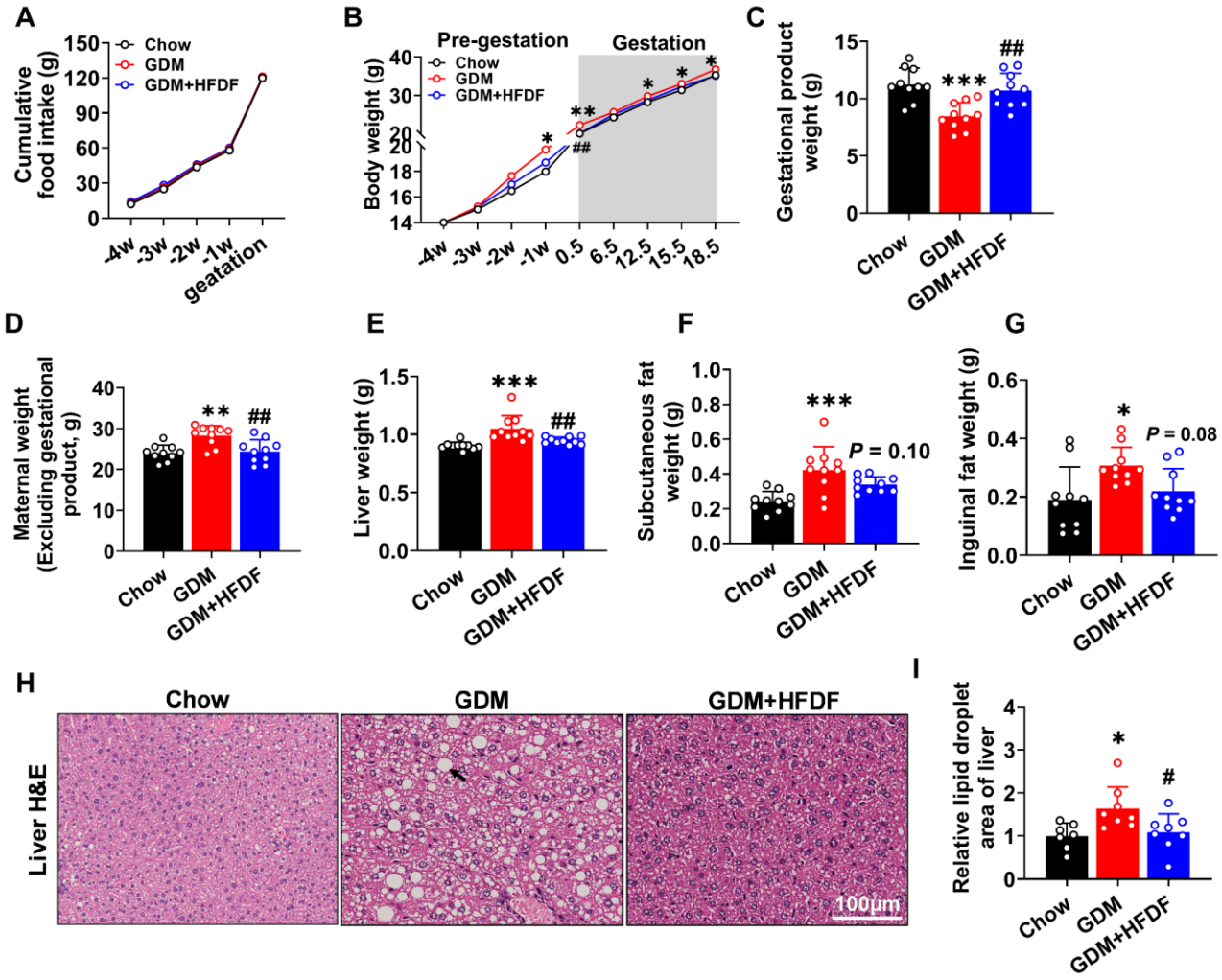

Fig. S2. Effect of HFDF on feed intake, maternal body weight, gestational product weight, liver weight and fat weight. (**A**) Cumulative food intake (n = 10 mice/group). (**B** to **G**) Body weight, gestational product weight (sum of placenta and fetus), maternal weight without gestational product (excluding placenta and fetus), liver weight, subcutaneous fat weight, and inguinal fat weight (n = 10 mice/group). (**H** and **I**) Representative H&E-staining images of accumulated hepatic lipids in liver sections and quantification (n = 6 mice/group). Data were analyzed by two-way ANOVA followed by post hoc Bonferroni tests (A and B) and one-way ANOVA followed by post hoc Tukey's tests (C to I), and represented mean ± SEM. **P* < 0.05, ***P* < 0.01, ****P* < 0.001, relative to the Chow group. #*P* < 0.05, ##*P* < 0.01, ###*P* < 0.001, relative to the GDM group.

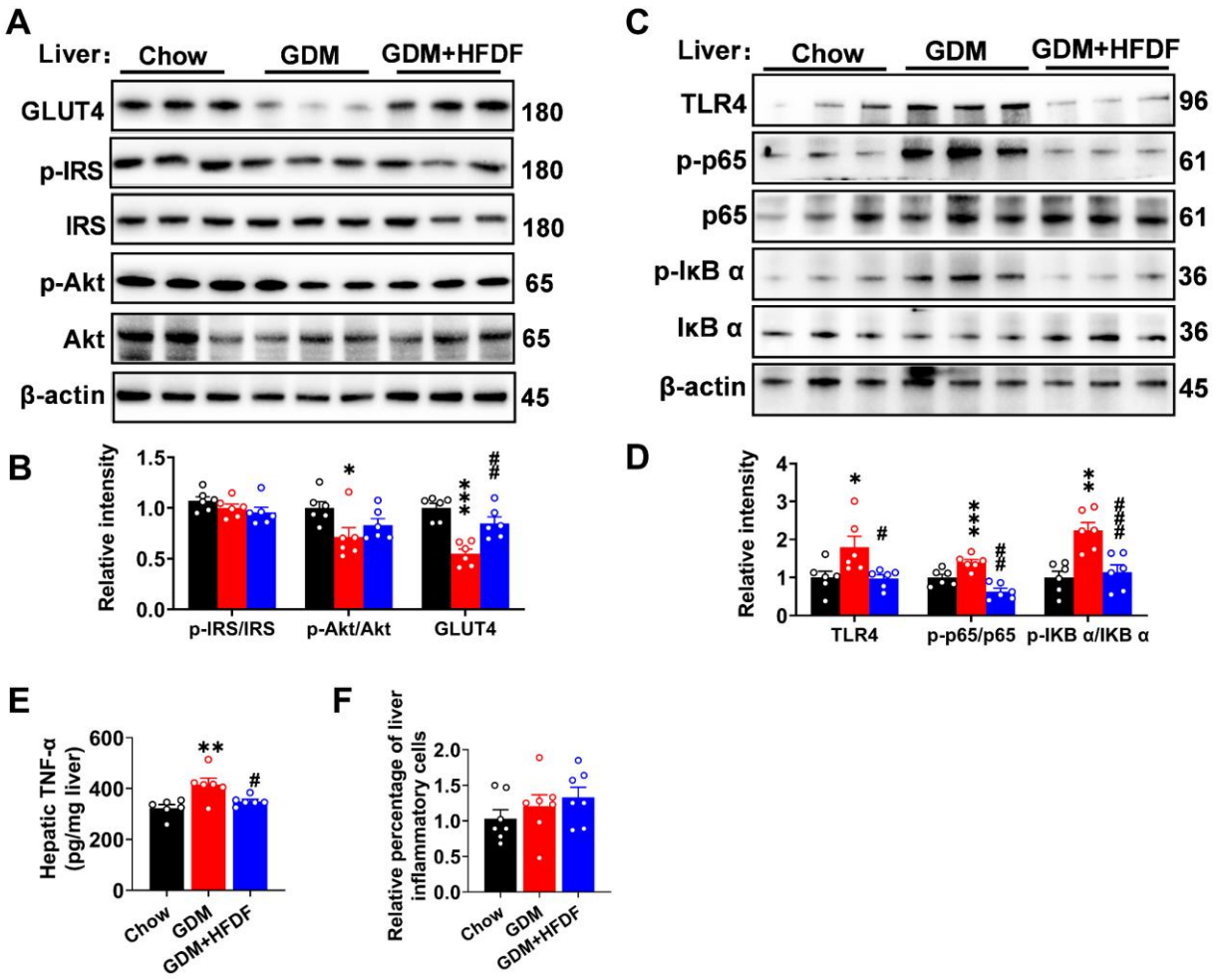

Fig. S3. Effects of HFDF on HFD-induced metabolic phenotype of liver at E18.5. (**A** to **D**) Immunoblots of insulin signaling pathway (GLUT4, p-IRS/IRS, and p-Akt/Akt), and TLR4/NF-κB inflammatory pathway (TLR4, p-p65/p65, and p-IκB α/ IκB α) in liver (n = 6 mice/group). (**E**) Hepatic TNF-α levels (n = 6 mice/group). (**F**) Statistical analysis of the percentage of hepatic inflammatory cells by H&E-staining (n = 6 mice/group). Data were analyzed by one-way ANOVA followed by post hoc Tukey's tests and represented mean ± SEM. *P* values were determined by **P* < 0.05, ***P* < 0.01, ****P* < 0.001, relative to the Chow group. #*P* < 0.05, ##*P* < 0.01, ###*P* < 0.001, relative to the GDM group.

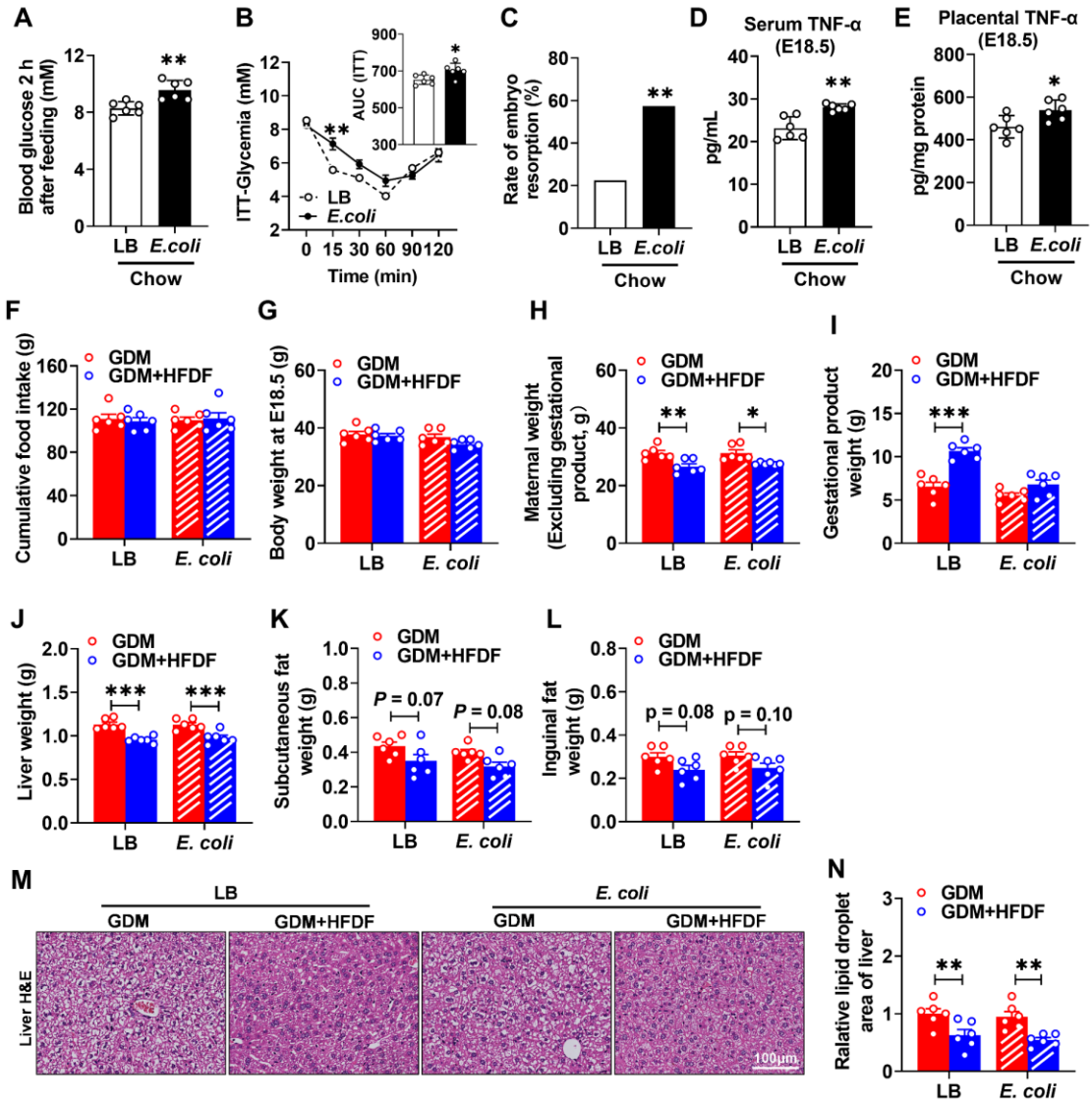

Fig. S4. Effects of *E. coli*-induced placental inflammation on maternal phenotype. (**A**) Blood glucose 2 h after feeding (n = 6 mice/group). (**B**) ITT and AUC (n = 6 mice/group). (**C**) Rate of embryo resorption at E18.5 (n = 6 litters/group). (**D** and **E**) Serum and placental TNF-α level in each group at E18.5 (n = 6 mice/group). (**F**) Cumulative food intake (n = 6 mice/group). (**G** to **L**) Body weight, maternal weight without gestational product (excluding placenta and fetus), gestational product weight (placenta and fetus), liver weight, subcutaneous fat weight, and inguinal fat weight at E18.5 (n = 6 mice/group). (**M** and **N**) Representative H&E-staining images of accumulated hepatic lipids in liver sections and quantification (n = 6 mice/group). Scale bars, 100 μm. Data were analyzed by unpaired Student's t-test (A, AUC, D, and E), two-way ANOVA followed by post hoc Bonferroni tests (F to N) and Chi-square test (C), and represented mean ± SEM. **P* < 0.05, ***P* < 0.01, ****P* < 0.001, relative to the LB or GDM group.

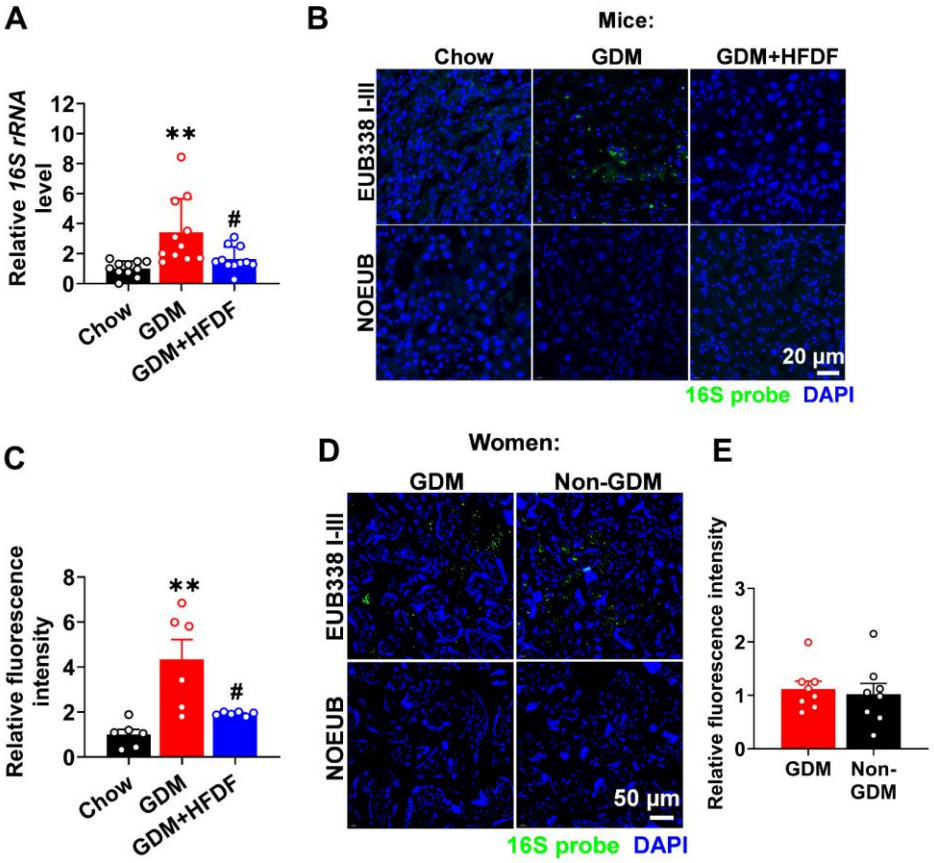

Fig. S5. Placental bacterial translocation in GDM model and women. (**A**) Comparison of total bacterial load in the placenta (n = 12 placentae from 6 litters per group). Six mice per group, and two placentae per mice. *16S rRNA* level of each sample was normalized to the average values of Chow group. (**B** and **C**) Representative images and *in situ* detection/quantification of bacteria in Chow, GDM, and GDM+HFDF placentae. Placental tissue sections were stained with DAPI (blue) and probed with universal eubacterial probe EUB338 I-III (16S probe, green) and scrambled probe NOEUB (n = 6 placentae from 6 litters per group). Scale bars, 20 μm. (**D** and **E**) Representative images and *in situ* detection/quantification of bacteria in GDM and Non-GDM women (n = 8). Scale bars, 50 μm. Data were analyzed by one-way ANOVA followed by post hoc Tukey's tests (A and C) or unpaired Student's t-test (E), and represented mean ± SEM. **P* < 0.05, ***P* < 0.01, ****P* < 0.001, relative to the Chow group. #*P* < 0.05, ##*P* < 0.01, ###*P* < 0.001, relative to the GDM group.

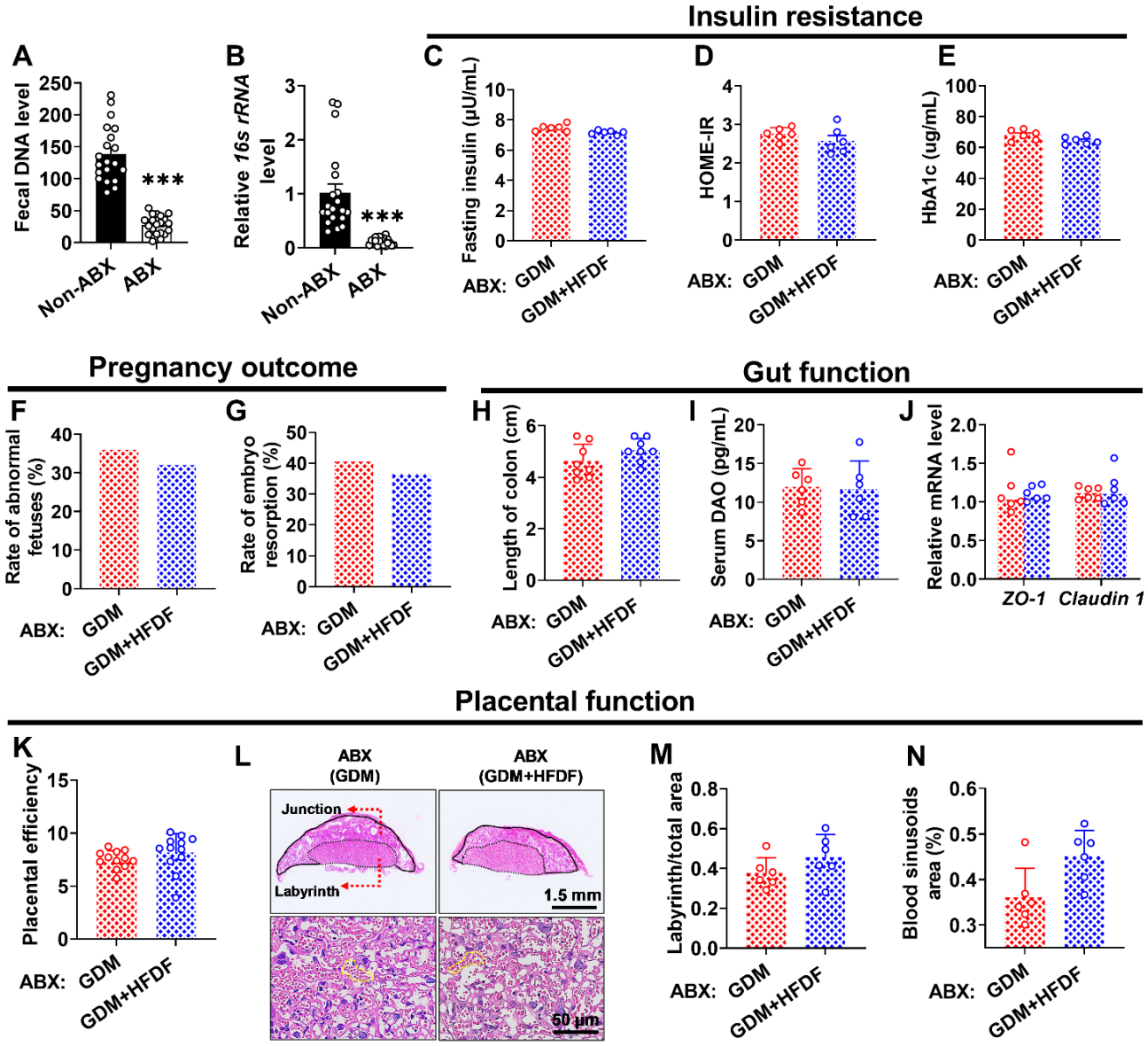

Fig. S6. Effects of HFDF on placental and gut phenotype after removal of gut microbes. Illustration of ABX experiment is shown **Fig. 7A**. At E18.5, serum, intestinal and placental samples were obtained after execution of mice (n = 10 mice/group). (**A** and **B**) Fecal DNA levels and total bacterial load after 14 days of antibiotic cocktail treatment (n = 20 mice/group). (**C**) Mice were fasted overnight and serum insulin level was measured (n = 6 mice/group). (**D**) HOMA-IR index (n = 6 mice/group). (**E**) Mice were fasted overnight and serum HbA1c level was measured (n = 6 mice/group). (**F** and **G**) Rates of abnormal fetuses and embryo resorption in each group (n = 10 litters/group). Abnormal fetuses are defined as macrosomia and intrauterine growth restriction fetuses. (**H**) Length of colon (n = 10 mice/group). (**I**) Serum DAO level (n = 6 mice/group). **(J)** Relative expression levels of barrier-forming tight junction-markers (*ZO-1* and *Claudin 1*) (n = 6 mice/group). (**K**) Placental efficiency was indicated by the ratio of fetal weight to placental weight (n = 10 litters/group). (**L** to **N**) Representative H&E-staining images of midsagittal placental tissue

sections used in histomorphological analysis. The labyrinth zone/junctional zone and typical blood sinusoid were marked with red arrows and yellow dotted line, respectively. The ratio between the labyrinth/total zones and the percentage of blood sinusoid area (n = 6 placentae from 6 litters per group) were measured. Scale bars, 1.5 mm and 50 μm. Data were analyzed by unpaired Student's t-test and represented mean ± SEM. ***$P < 0.001$, relative to the Non-ABX group.

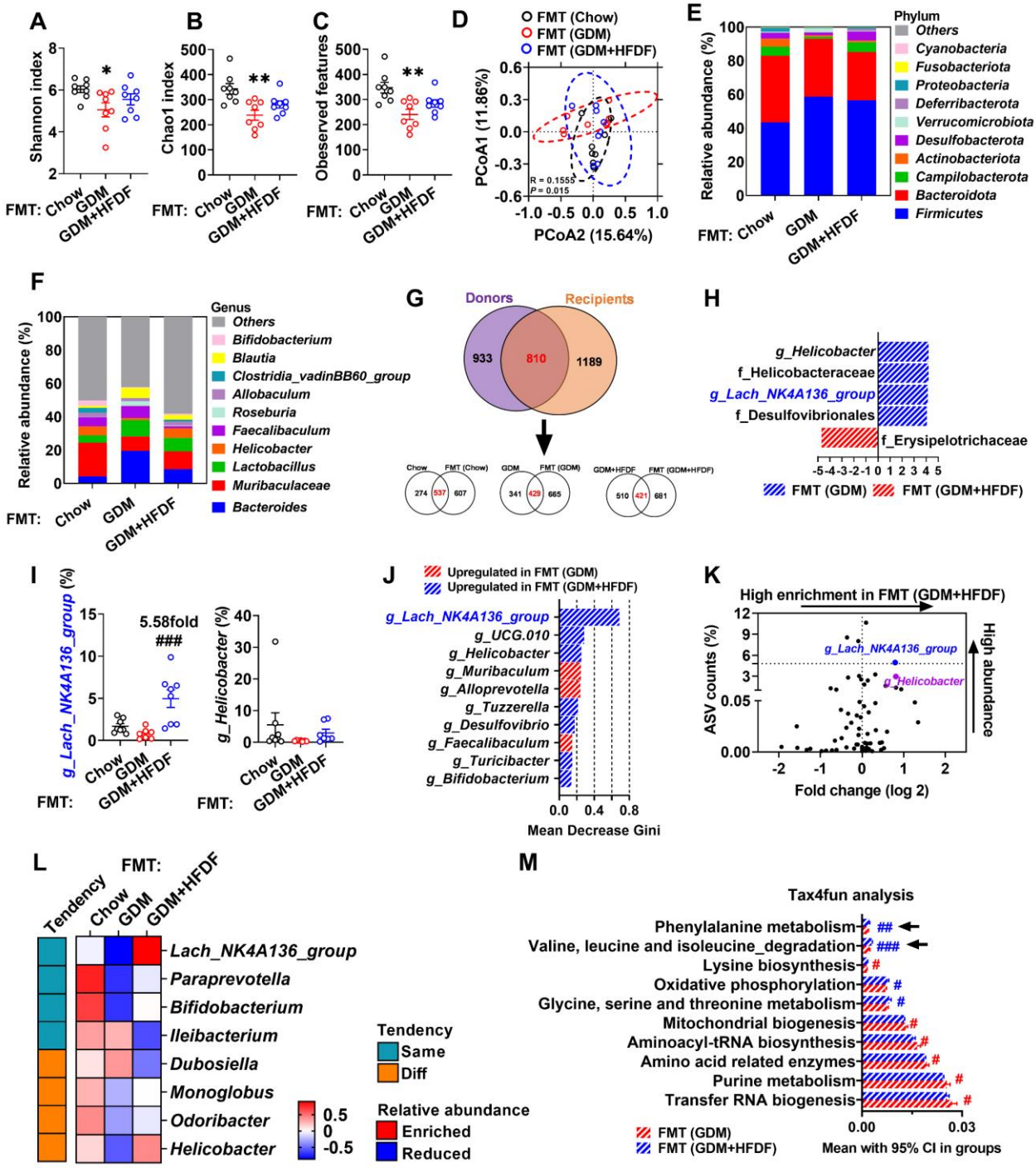

Fig. S7. Post-transplanted intestinal microbial profiles of recipient mice. Illustration of FMT experiment is shown **Fig. 7H**. At E18.5, fresh feces of recipient mice were obtained, followed by *16S rRNA* analysis (n = 8 mice/group). (**A** to **C**) Alpha-diversity indices, including Shannon, Chao1, and observed features between FMT (Chow), FMT (GDM), and FMT (GDM+HFDF) (n = 8 mice/group). (**D**) PCoA based on bray-curtis between FMT (Chow), FMT (GDM), and FMT (GDM+HFDF) (n = 8 mice/group). (**E** and **F**) Average relative abundances of predominant taxa at the phylum level (E) and genus level (F) (n = 8 mice/group). (**G**) Venn diagram for comparing the shared ASV number in the gut microbiome of different comparison groups. (**H**) The most

differentially abundant taxa between the three groups as identified by LDA effect size (n = 8 mice/group). Enriched taxa in FMT (GDM) and FMT (GDM+HFDF) are indicated by red and blue bars, respectively. Only LDA threshold ≥ 4 taxa are shown. (**I**) Relative abundances of *g_ Lachnospiraceae _NK4A136_group* and *g_Helicobacter* (n = 7-8 mice/group). (**J**) Identification of key bacterial genera by the random forest method using the *16S rRNA* gene sequencing data of FMT (GDM) and FMT (GDM+HFDF) groups. Higher Mean Decrease Gini values indicate greater importance of the variable. (**K**) Volcano plot for relative abundance distribution of microbial ASVs. Each symbol represents one mouse or bacterial taxa. (**L**) Heat map for comparing the abundance of altered genera between mice donors and recipient mice. Red, more abundant; blue, less abundant. Genera with a trend consistent with the variation in donors are marked with green points, while those with an inconsistent trend are marked with yellow points. (**M**) Relative abundance of metabolic pathways (top 10) in gut predicted by Tax4fun (n = 8 mice/group). Data were represented means ± SEM or means with 95% CI. *P* values were determined by one-way ANOVA followed by post hoc Tukey's tests (A to C), one-way ANOVA followed by Two-stage step-up FDR method of Benjamini, Krieger and Yekutieli (I), or unpaired Student's t-test (M). **P* < 0.05, ***P* < 0.01, relative to FMT (Chow) group. #*P* < 0.05, ##*P* < 0.01, ###*P* < 0.001, relative to FMT (GDM) group.

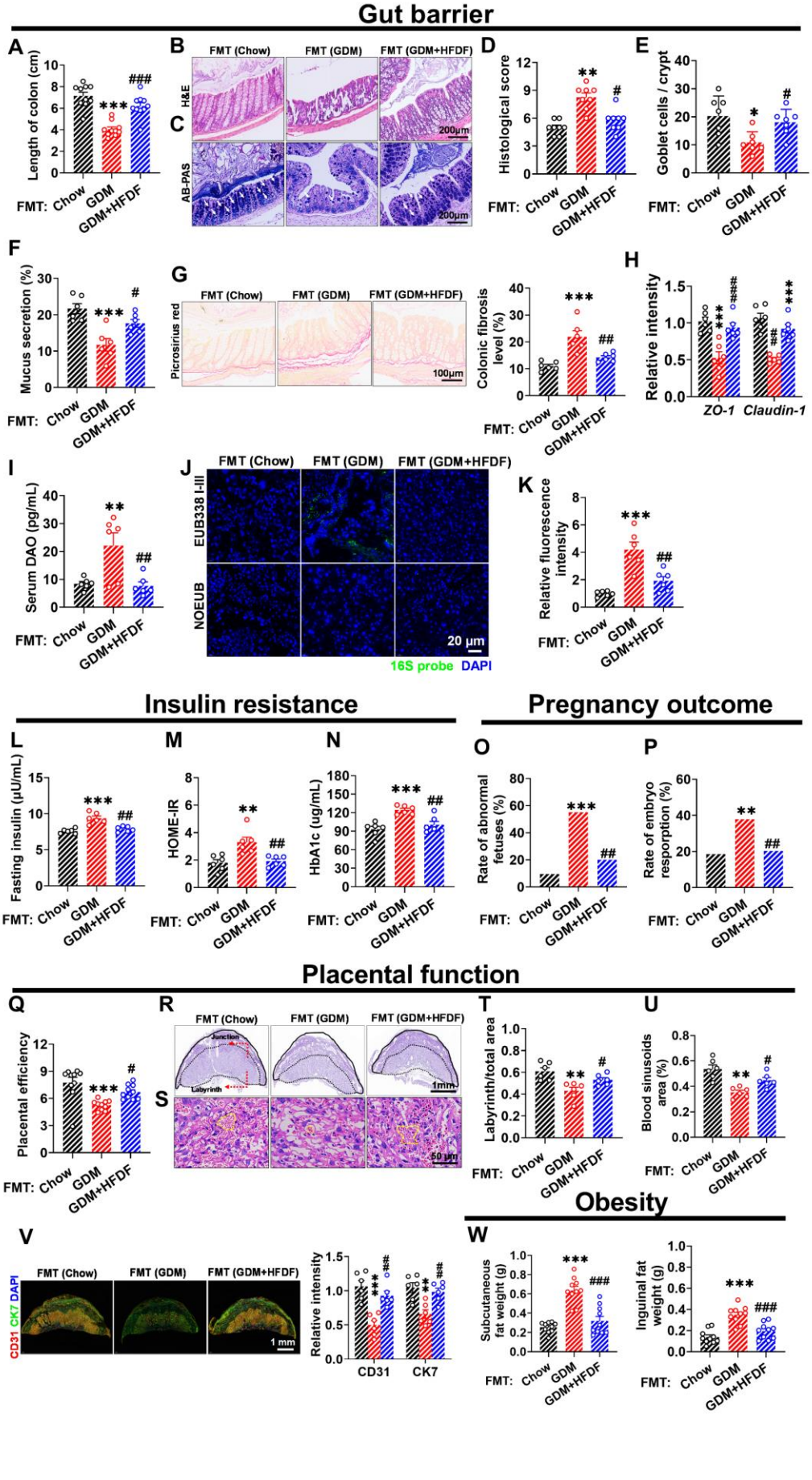
Gut barrier
A
Length of colon (cm)
FMT: Chow
GDM
GDM+HFDF
B
FMT (Chow)
FMT (GDM)
FMT (GDM+HFDF)
H&E
AB-PAS
200μm
C
D
Histological score
E
Goblet cells / crypt
F
Mucus secretion (%)
G
Picrosirius red
100μm
Colonic fibrosis level (%)
H
Relative intensity
ZO-1
Claudin-1
I
Serum DAO (pg/mL)
J
EUB338 I-III
NOEUB
20 μm
16S probe
DAPI
K
Relative fluorescence intensity
Insulin resistance
L
Fasting insulin (μU/mL)
M
HOME-IR
N
HbA1c (ug/mL)
Pregnancy outcome
O
Rate of abnormal fetuses (%)
P
Rate of embryo resorption (%)
Placental function
Q
Placental efficiency
R
Junction
Labyrinth
1mm
S
50 μm
T
Labyrinth/total area
U
Blood sinusoids area (%)
V
CD31
CK7
DAPI
1 mm
Relative intensity
CD31
CK7
Obesity
W
Subcutaneous fat weight (g)
Inguinal fat weight (g)

Fig. S8. Effects of FMT on HFD-induced impairment of gut barrier function, insulin resistance, pregnancy outcomes, placental function, and obesity. Illustration of FMT experiment is shown **Fig. 7H**. (**A**) Length of colon (n = 10 mice/group). (**B**, **D**, and **E**) Representative H&E-staining images of the colon sections, histological score, and goblet cell number per colonic crypt (n = 7 or 8 mice/group). Scale bars, 200 μm. (**C** and **F**) Representative AB-PAS-staining images of colon sections and quantification of mucus secretion (n = 6 mice/group). Typical mucus was marked with white arrows. Scale bars, 200 μm. (**G**) Representative Picrosirius red of colon sections and quantification (n = 6 mice/group). Scale bars, 100 μm. (**H**) Relative mRNA expression levels of barrier-forming tight junction-markers (*ZO-1* and *Claudin-1*) (n = 6 mice/group). (**I**) Serum DAO level (n = 6 mice/group). (**J** and **K**) Representative images and *in situ* detection/quantification in placentae (n = 6 placentae from 6 litters per group). Scale bars, 20 μm. (**L** to **N**) Serum insulin and HbA1c levels, and HOME-IR (n = 6 mice/group). (**O** and **P**) Rates of abnormal fetuses and embryo resorption (n = 10 litters/group). (**Q**) Placental efficiency was indicated by the ratio of fetal weight to placental weight (n = 10 litters per group). (**R** to **U**) Representative H&E staining images of midsagittal placental tissue sections (n = 6 placentae from 6 litters per group). The labyrinth zone and junction zone were marked with black arrows and the typical blood sinusoid was marked with yellow dotted line. Scale bars, 1 mm and 50 μm. (**V**) Immunofluorescence and quantification of placental function-related factors (CD31 and CK7) (n = 6 placentae from 6 litters per group). (**W**) Subcutaneous and inguinal fat weight (n = 10 mice/group). Data were analyzed by one-way ANOVA followed by post hoc Tukey's tests (A-N and Q-W) or Chi-square test (O and P), and represented mean ± SEM. **P* < 0.05, ***P* < 0.01, ****P* < 0.001, relative to the FMT (Chow) group. #*P* < 0.05, ##*P* < 0.01, ###*P* < 0.001, relative to the FMT (GDM) group.

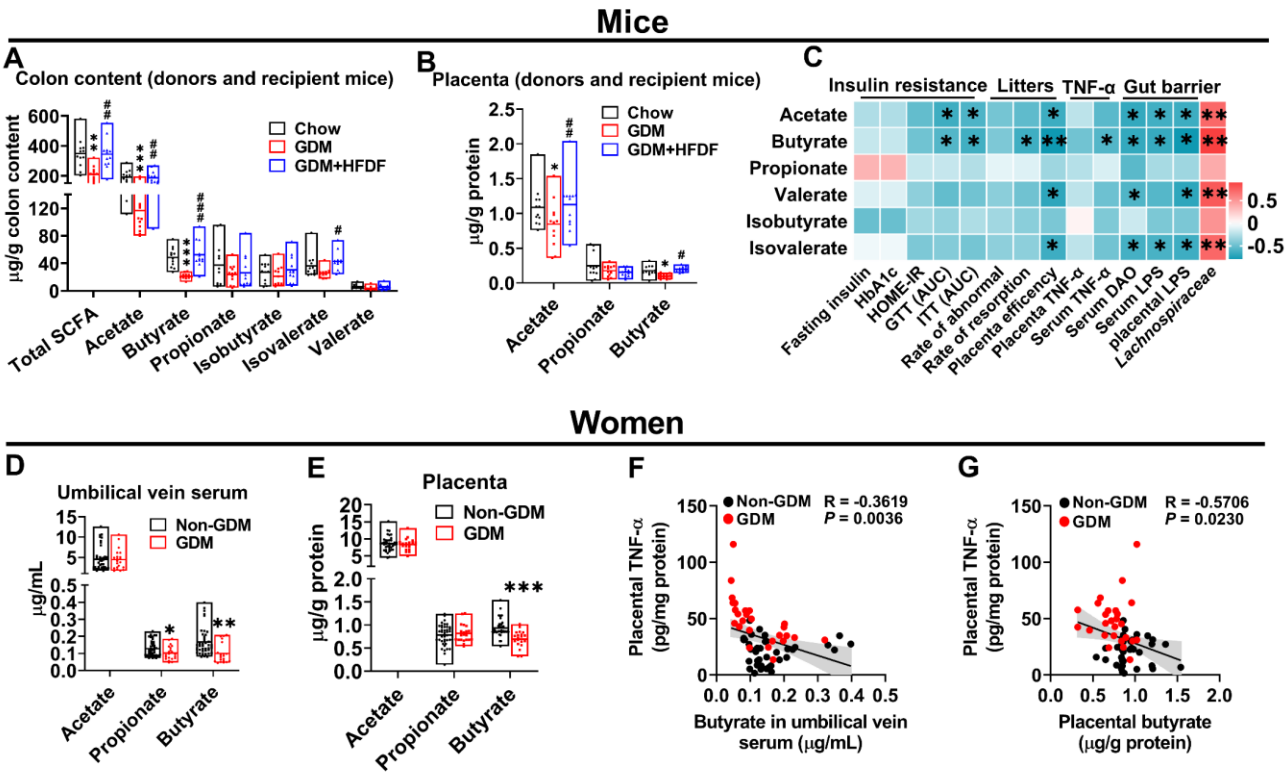

Fig. S9. SCFAs levels in mice and pregnant women. (**A** and **B**) SCFA levels in colon content and placenta of mice donors and recipient mice at E18.5 (n = 12 mice/group). (**C**) Two-tailed Pearson's correlation coefficient analysis between SCFA levels and insulin resistance, litters, TNF-α, or gut barrier parameters in donors. These parameters are based on data from Figures 2-5 and 7. (**D** and **E**) Comparison of SCFA levels in the umbilical vein serum and placenta of Non-GDMs (n = 42) and GDMs (n = 21). Isobutyrate, isovalerate and valerate levels were not presented because they were below the detection limit. (**F** and **G**) Two-tailed Pearson's correlation coefficient analysis of placental TNF-α levels and SCFA levels in the umbilical vein serum, and placenta. Data were analyzed by one-way ANOVA followed by post hoc Tukey's tests (A and B) or unpaired Student's t-test (D and E), and represented mean ± SEM. *, #$P < 0.05$, **, ##$P < 0.01$, ***, ###$P < 0.001$, with * vs Chow or Non-GDM, # vs GDM.

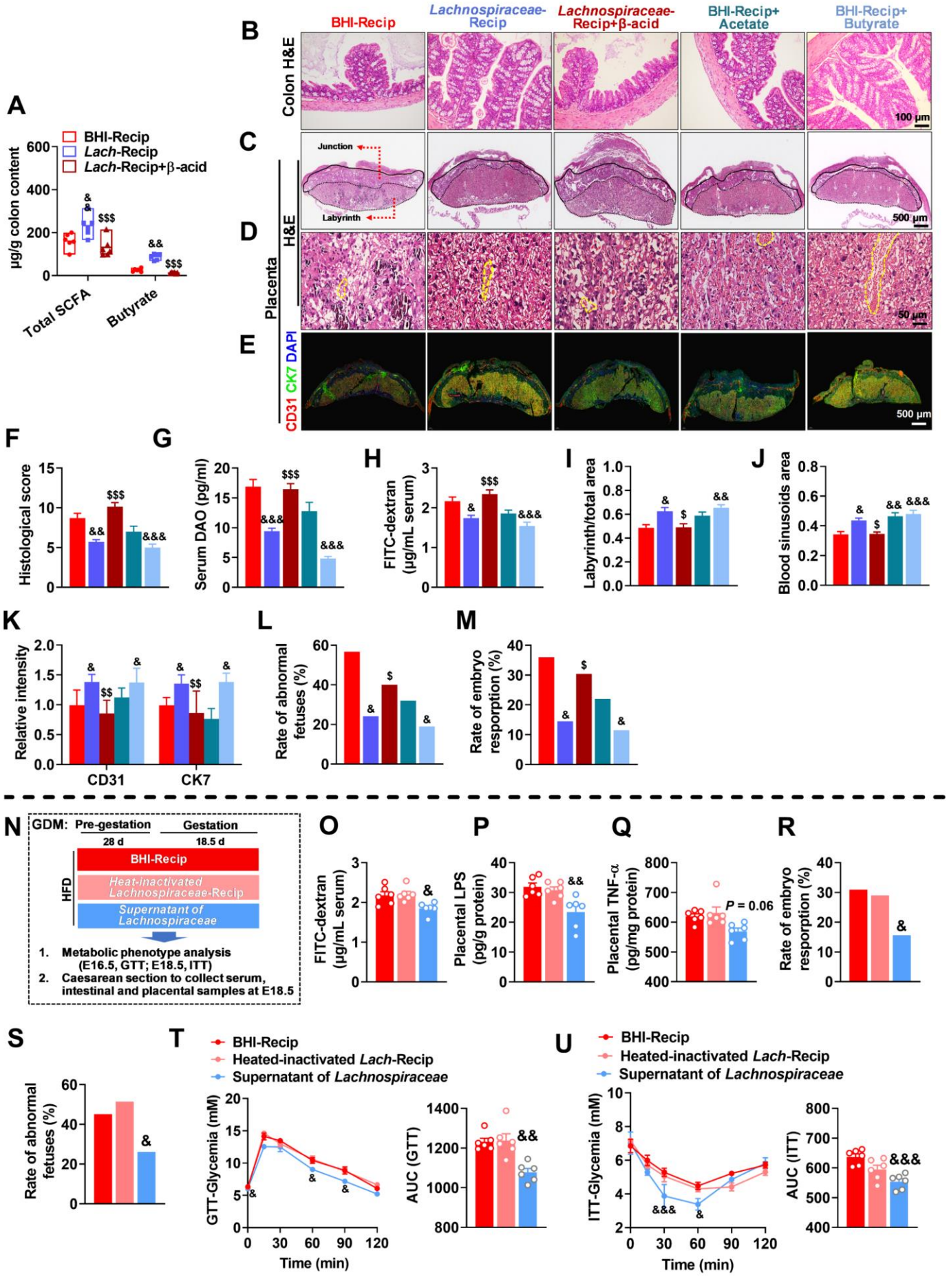
A
BHI-Recip
Lach-Recip
Lach-Recip+β-acid
μg/g colon content
Total SCFA
Butyrate
B
BHI-Recip
Lachnospiraceae-Recip
Lachnospiraceae-Recip+β-acid
BHI-Recip+Acetate
BHI-Recip+Butyrate
Colon H&E
100 μm
C
Junction
Labyrinth
H&E
500 μm
D
Placenta
50 μm
E
CD31 CK7 DAPI
500 μm
F
Histological score
G
Serum DAO (pg/ml)
H
FITC-dextran (μg/mL serum)
I
Labyrinth/total area
J
Blood sinusoids area
K
Relative intensity
CD31
CK7
L
Rate of abnormal fetuses (%)
M
Rate of embryo resorption (%)
N
GDM: Pre-gestation 28 d
Gestation 18.5 d
HFD
BHI-Recip
Heat-inactivated Lachnospiraceae-Recip
Supernatant of Lachnospiraceae
1. Metabolic phenotype analysis (E16.5, GTT; E18.5, ITT)
2. Caesarean section to collect serum, intestinal and placental samples at E18.5
O
FITC-dextran (μg/mL serum)
P
Placental LPS (pg/g protein)
Q
Placental TNF-α (pg/mg protein)
P = 0.06
R
Rate of embryo resorption (%)
S
Rate of abnormal fetuses (%)
T
BHI-Recip
Heated-inactivated Lach-Recip
Supernatant of Lachnospiraceae
GTT-Glycemia (mM)
Time (min)
AUC (GTT)
U
BHI-Recip
Heated-inactivated Lach-Recip
Supernatant of Lachnospiraceae
ITT-Glycemia (mM)
Time (min)
AUC (ITT)

Fig. S10. Effects of *Lachnospiraceae* and SCFAs on HFD-induced GDM phenotype and impairment of gut barrier function, placental function, and pregnancy outcome. Illustration of this experiment is shown in Fig. 8A. (**A**) SCFA levels in colon content of E18.5 mice (n = 6 mice/group). (**B** and **F)** Representative H&E staining images of colon sections and histological score (n = 6 mice/group). Scale bars, 100 μm. (**C**, **D**, **I**, and **J**) Representative H&E-staining images of midsagittal placental tissue sections used for histomorphological analysis, with labyrinth zone and junctional zone marked and indicated by red arrows. Typical blood sinusoid was marked with yellow dotted line. The ratio between the labyrinth/total zones and the percentage of blood sinusoid area were measured (n = 6 placentae from 6 litters per group). Scale bars, 500 μm and 50 μm. (**E** and **K**) Immunofluorescence and quantification of placental function-related factors (CD31 and CK7) (n = 6 placentae from 6 litters per group). (**G**) Serum DAO levels (n = 6 mice/group). (**H** and **O**) Serum FITC-dextran levels (n = 6 mice/group). (**L**, **M**, **R**, and **S**) Rates of abnormal fetuses or embryo resorption (n = 6 litters/group). (**N**) Schematic of medium control (BHI), heat-inactivated *Lachnospiraceae*, and culture supernatants of live *Lachnospiraceae* treatments in GDM model. (**P** and **Q**) Placental LPS and TNF-αlevels (n = 6 placentae from 6 litters per group). (**T** and **U**) GTT, ITT, and AUC (n = 6 mice/group). Data were analyzed by one-way ANOVA followed by post hoc Tukey's tests (A to K, O to Q, and AUC), Chi-square test (L, M, R and S) or two-way ANOVA followed by post hoc Bonferroni tests (GTT and ITT), and represented mean ± SEM or mean. &, $$P < 0.05$, &&, $$$P < 0.01$, &&&, $$$$P < 0.001$, with & vs BHI-Recip, $ vs *Lachnospiraceae*-Recip.

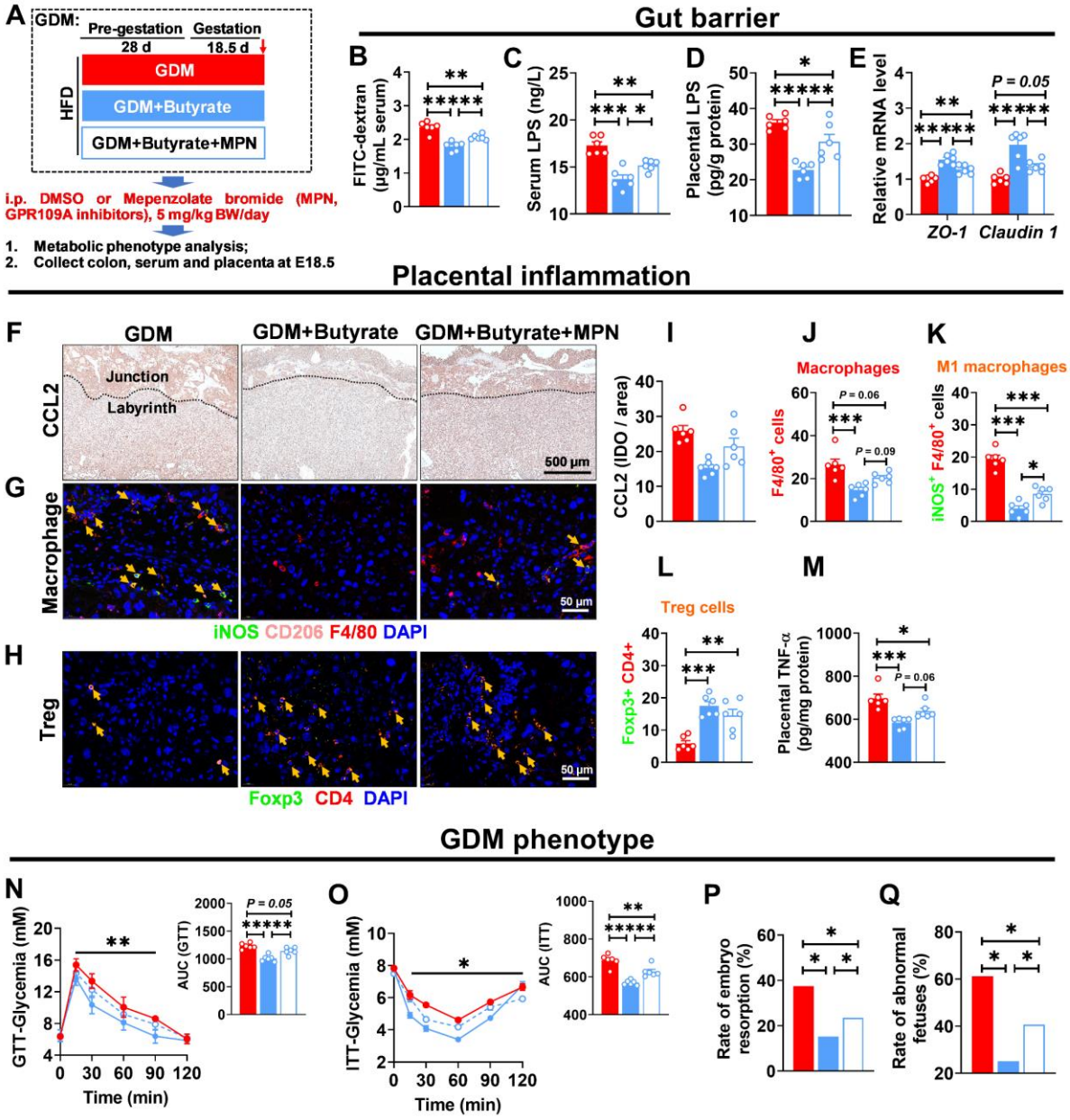

Fig. S11. Role of GPR109A in butyrate-mediated alleviation of barrier function impairment and placental inflammation in GDM model. (**A**) Schematic of butyrate and MPN (a specific inhibitor of GPR109A) treatments in GDM model. HFD-fed mice were supplemented with butyrate in drinking water (200 mM) and intraperitoneally injected with MPN (5 mg/kg/day), a specific inhibitor of GPR109A, during pre-gestation and post-gestation. Intraperitoneal GTT and ITT tests were performed at E16.5 and E18.5, respectively. At E18.5, serum, intestinal and placental samples were obtained after execution of mice (n = 6 mice/group). (**B** and **C**) Serum LPS and FITC-dextran levels (n = 6 mice/group). (**D** and **M**) Placental LPS and TNF-α levels (n = 6 placentae from 6 litters per group). (**E**) Relative mRNA expression levels of barrier-forming tight junction-markers (*ZO-1* and *Claudin 1*) in colon (n = 6 mice/group). (**F** and **I**) Immunohistochemistry and quantification of

CCL2 (one of the key factors in macrophage recruitment) in placenta (n = 6 placentae from 6 litters per group). Scale bars, 500 μm. (**G**, **J**, and **K**) Localization of macrophage (F4/80+, red), M1 macrophage (iNOS+/F4/80+, green/red; yellow arrow), and M2 macrophage ($CD206^+$ $F4/80^+$, pink/red; it was not quantified because it was almost non-existent) in placenta by immunofluorescence (n = 6 placentae from 6 litters per group). Scale bars, 50 μm. (**H** and **L**) Localization of Treg cell（$Foxp3^+/CD4^+$; yellow arrow) in placenta by immunofluorescence (n = 6 placentae from 6 litters per group). Scale bars, 50 μm. (**N** and **O**) GTT, ITT, and AUC (n = 6 mice/group). (**P** and **Q**) Rates of abnormal fetuses and embryo resorption (n = 6 litters/group). Data were analyzed by one-way ANOVA followed by post hoc Tukey's tests (B to M, and AUC), Chi-square test (P and Q) or two-way ANOVA followed by post hoc Bonferroni tests (GTT and ITT), and represented mean ± SEM. $*P < 0.05$, $**P < 0.01$, $***P < 0.001$.

For Fig. 3I

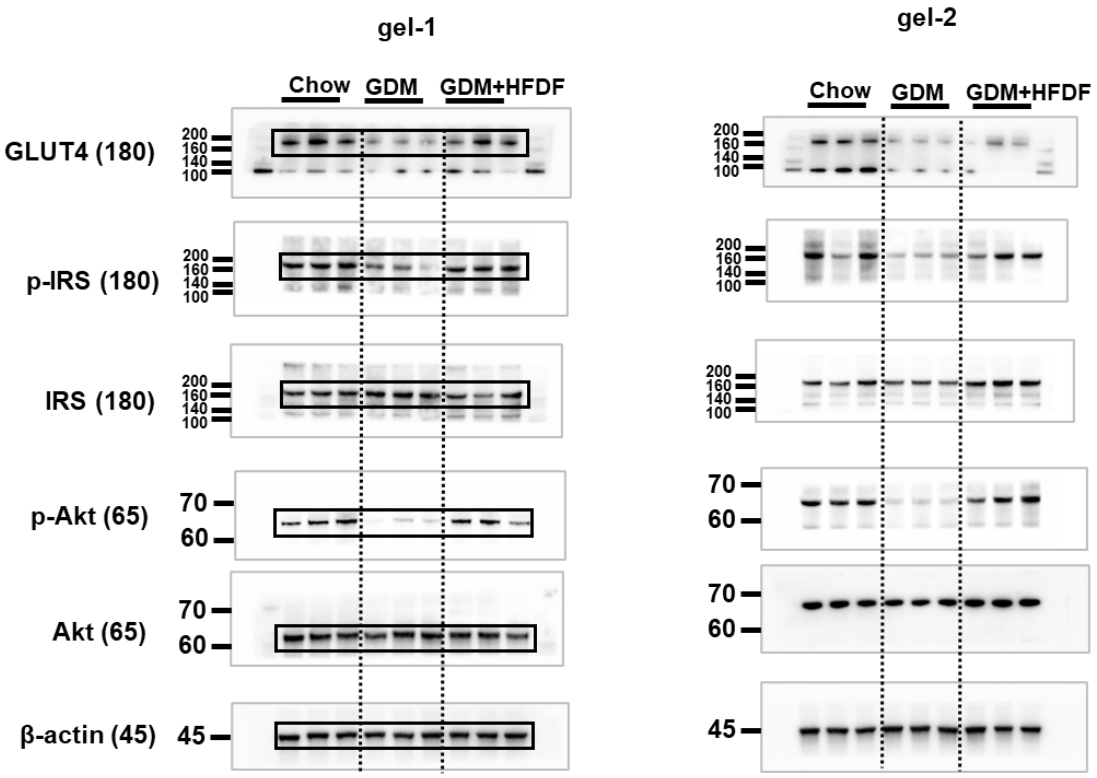

For Fig. 3K

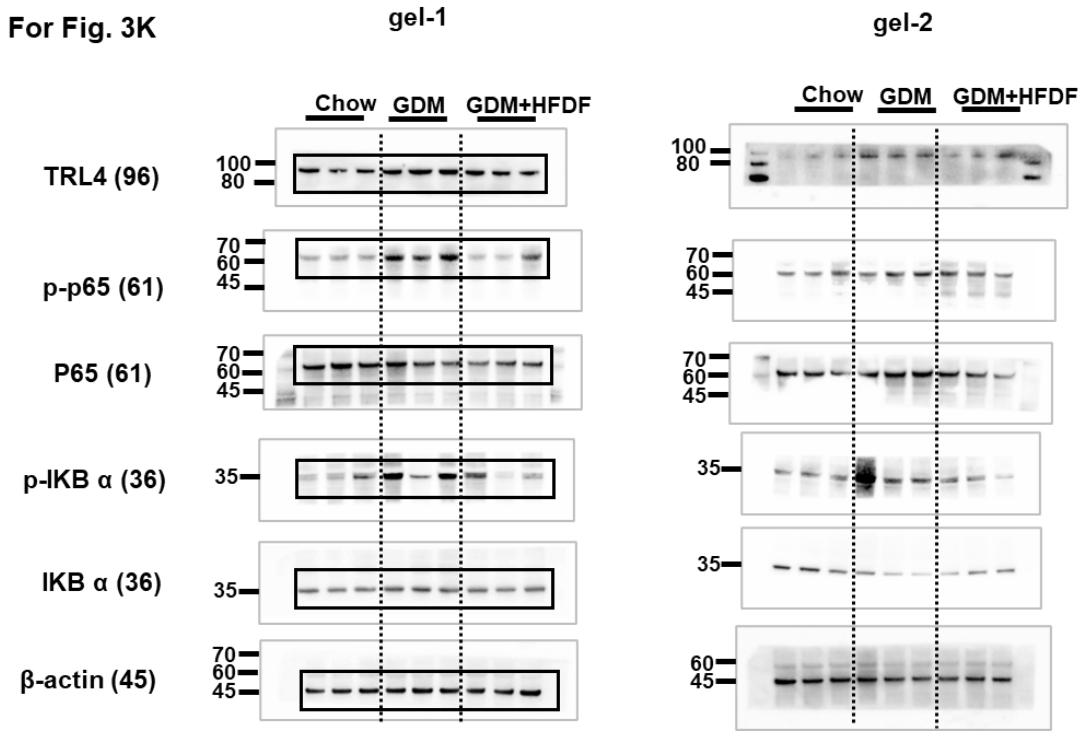

For Fig. 4F

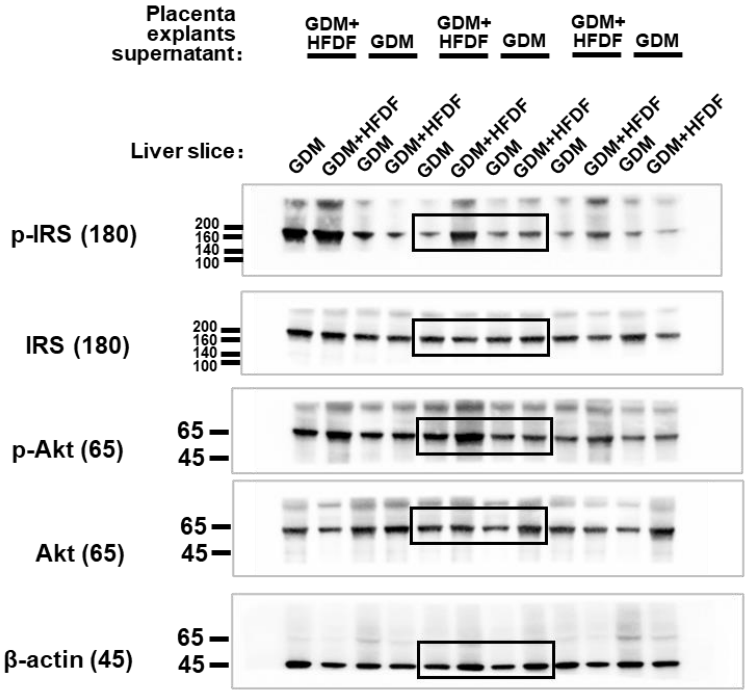

For Fig. 4N

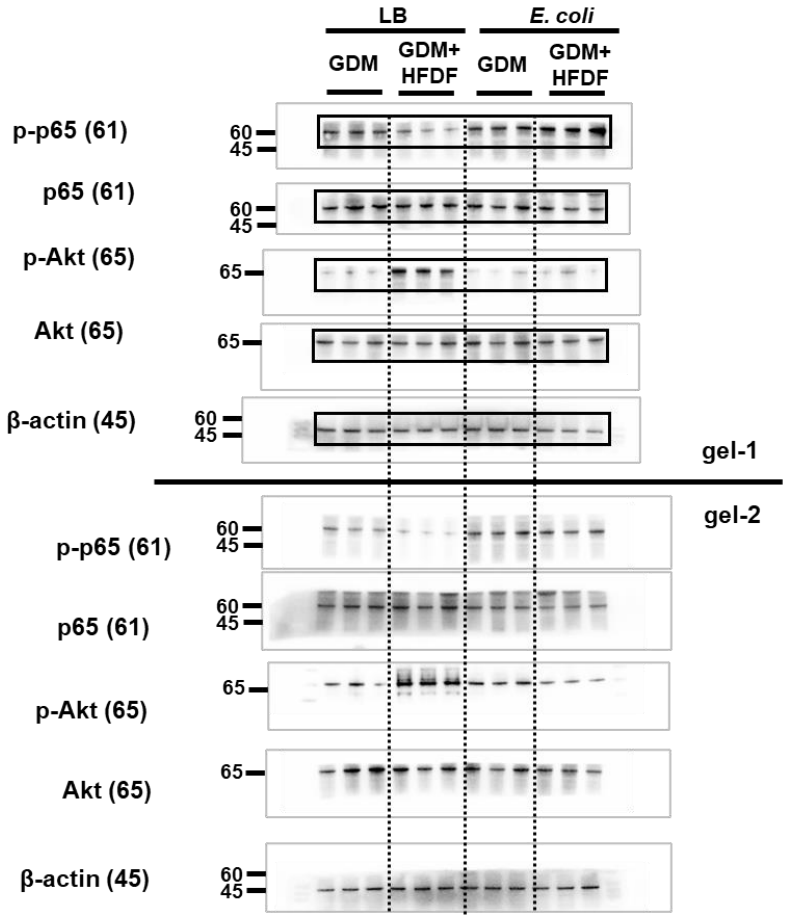

For Fig. 5L

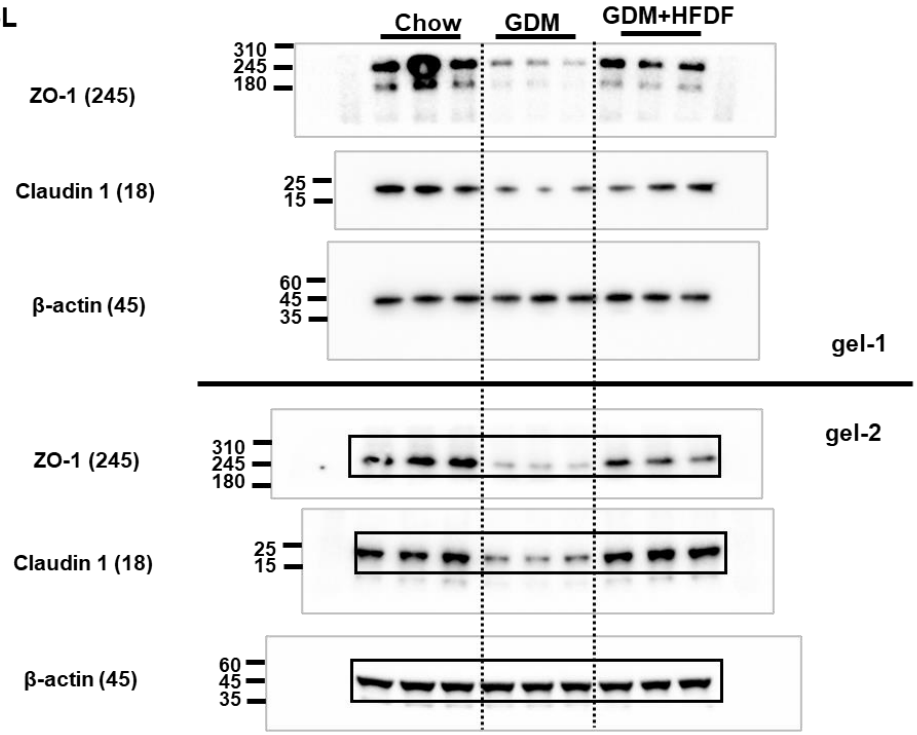

For Fig. 5N

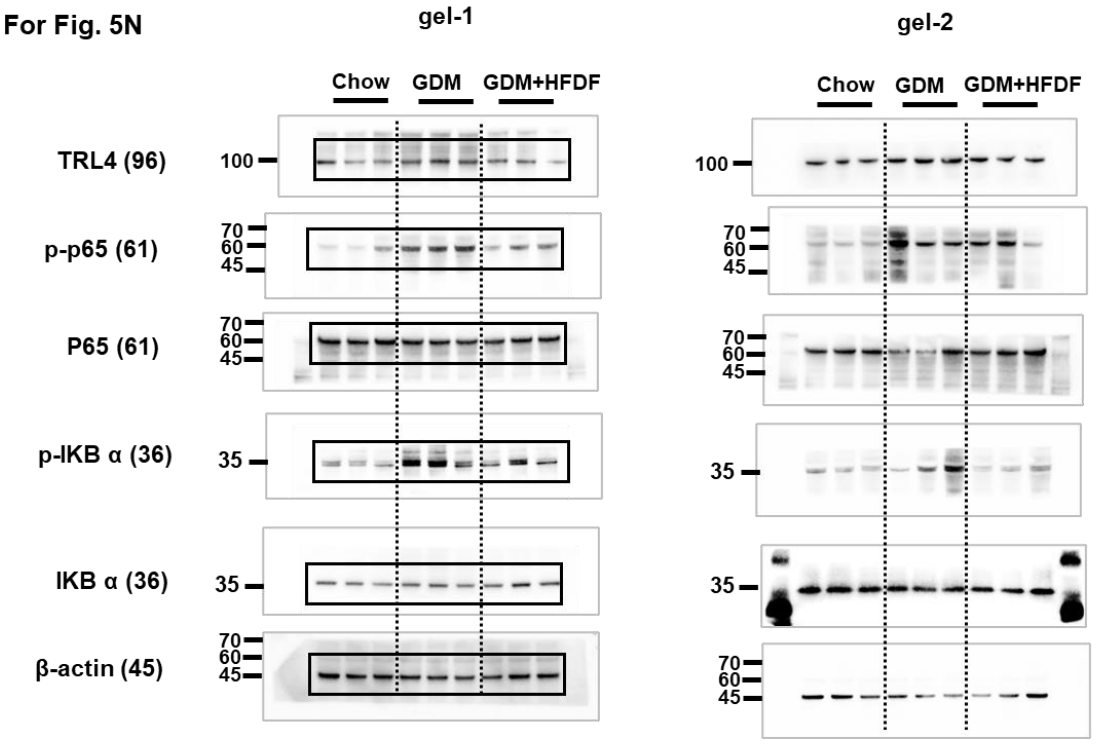

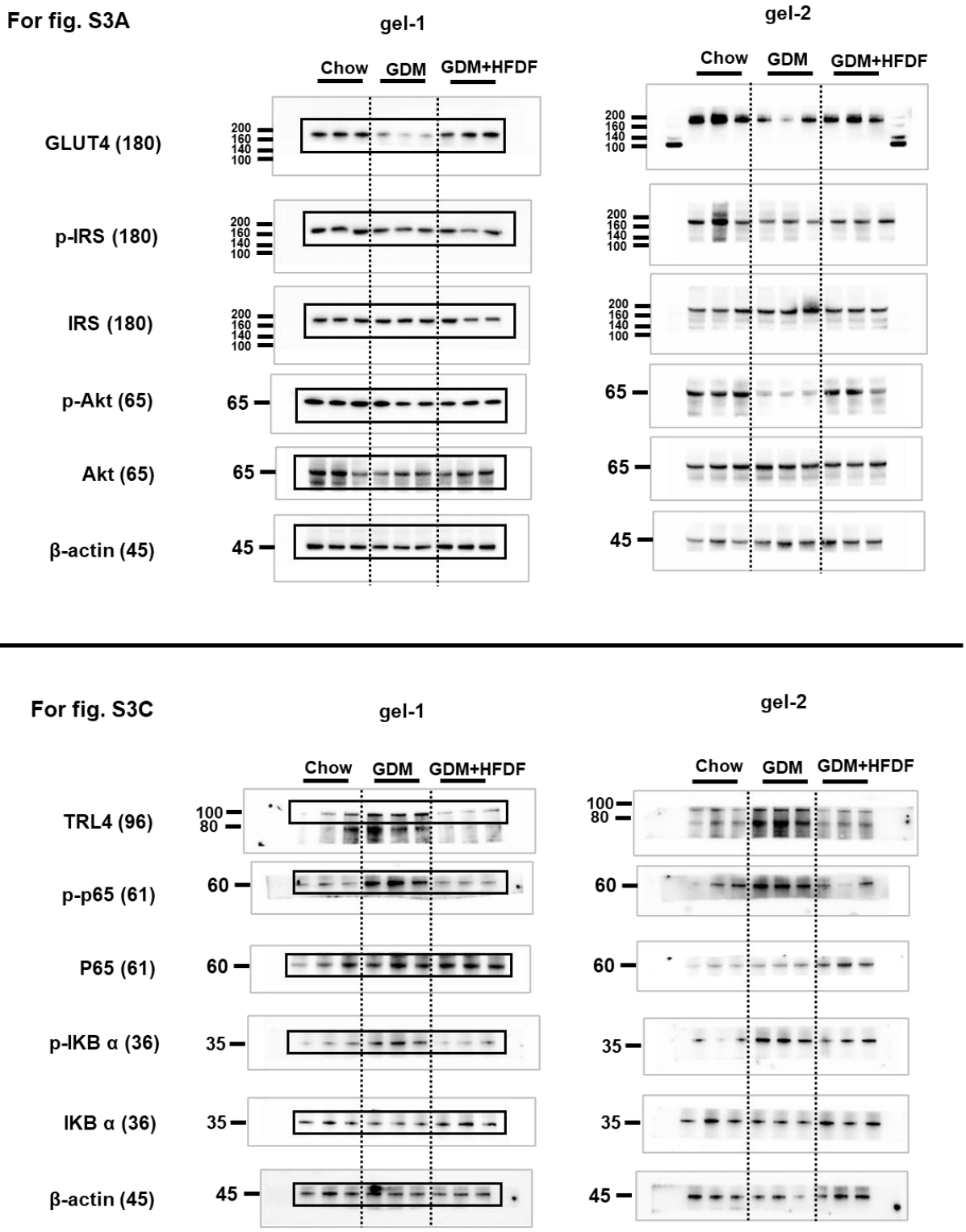

Fig. S12. Unedited western blots. Parts indicated with rectangles were included in the figure.

Table S1. Maternal, neonatal, and placental characteristics

Characteristics	GDMs (n = 21)	Non-GDMs (n = 42)	*P*
Maternal			
Parity	1.76±0.94	2.14±1.18	0.58
Age (year)	34.24±3.36	31.33±4.80	0.02
Body mass index (kg/m^2)	24.31±3.29	20.58±2.54	< 0.01
SBP (mmHg)	114.14±15.97	115.10±17.00	0.56
DBP (mmHg)	75.12±10.84	74.52±12.59	0.72
OGTT at 28 weeks' gestation (mmol/L)			
Fasting	4.63±1.17	-	-
1h	9.99±2.79	-	-
2h	8.57±2.19	-	-
Neonatal			
Gestational age (week)	38.43±1.25	37.17±2.64	0.04
Birth weight (kg)	3.12±0.51	2.70±0.64	0.01
Sex, male/female	10/11	27/15	0.28
Placental vasculopathy (number, %)			
Placental inflammatory	18 (85.71%)	19 (45.24%)	< 0.01
Vascular infarction	15 (71.43%)	18 (42.86%)	0.04
Villous fibrinoid necrosis	10 (47.62%)	16 (38.10%)	0.63
Syncytial knots	9 (42.86%)	12 (28.57%)	0.28
Delivery mode, vaginal birth/caesarean section	19/2	36/6	0.71

GDMs, gestational diabetes mellitus patients; SBP, systolic blood pressure; DBP, diastolic blood pressure; OGTT, oral glucose tolerance test. Data represent the mean ± standard deviation or the mean. *P*-values were determined by unpaired Student's t-test, except for neonatal sex, placental vasculopathy and delivery mode, which were determined by Fisher's exact test for *P*-values.

Table S2. Diet composition of mice

Items	Chow	GDM	GDM+HFDF
Composition (% (w/w))			
Casein	19.0	25.8	25.8
Corn Starch	48.0	-	-
Maltodextrin	11.8	16.2	16.2
Sucrose	6.5	8.9	8.9
Soybean Oil	2.4	3.2	3.2
Pork oil	1.9	31.7	31.7
Mixed minerals	0.9	1.3	1.3
$CaHPO_4$	1.2	1.7	1.7
$CaCO_3$	0.5	0.7	0.7
Potassium citrate	1.6	2.1	2.1
Mixed Vitamins	0.9	1.3	1.3
Cysteine	0.3	0.4	0.4
Choline bitartrate	0.2	0.3	0.3
Dietary fiber			
Cellulose	4.7	6.5	-
Konjac flour	-	-	6.5
Energy			
AFE (kcal AFE/kg)	3845.5	5243.21	5243.21
AFE from fat (% kcal)	10.0	60.0	60.0
AFE from protein (% kcal)	20.0	20.0	20.0
AFE from carbohydrate (% kcal)	70.0	20.0	20.0

AFE, atwater fuel energy; GDM, gestational diabetes mellitus; HFD, high fat diet; HFDF, high fermentable dietary fiber.

Table S3. Key resource table

Reagent	Resource	Identifier
Oligonucleotides		
Primers for mice *β-actin* Forward: GTCCCTCACCCTCCCAAAAG Reverse: GCTGCCTCAACACCTCAACCC	Sangon Biotech	N/A
Primers for mice *16sRNA* Forward: GTGSTGCAYGGYTGTCGTCA Reverse: ACGTCRTCCMCACCTTCCTC	Sangon Biotech	N/A
Primers for mice *Ccl2* Forward: GCCTGCTGTTCACAGTTGC Reverse: GAGTGGGGCGTTAACTGCAT	Sangon Biotech	N/A
Primers for mice *Ccl3* Forward: TGTACCATGACACTCTGCAAC Reverse: CAACGATGAATTGGCGTGGAA	Sangon Biotech	N/A
Primers for mice *Csf3* Forward: CCTGGAGCAAGTGAGGAAGA Reverse: TGCAGGAGACCTTGGTAGAG	Sangon Biotech	N/A
Primers for mice *Cxcl1* Forward: ACTGCACCCAAACCGAAGTC Reverse: TGGGGACACCTTTTAGCATCTT	Sangon Biotech	N/A
Primers for mice *Cxcl2* Forward: CCAACCACCAGGCTACAGG Reverse: GCGTCACACTCAAGCTCTG	Sangon Biotech	N/A
Primers for mice *IL1β* Forward: GAAATGCCACCTTTTGACAGTG Reverse: TGGATGCTCTCATCAGGACAG	Sangon Biotech	N/A
Primers for mice *IL6* Forward: TCTATACCACTTCACAAGTCGGA Reverse: GAATTGCCATTGCACAACTCTTT	Sangon Biotech	N/A
Primers for mice *IL17A* Forward: GGCCCTCAGACTACCTCAAC Reverse: TCTCGACCCTGAAAGTGAAGG	Sangon Biotech	N/A

Primers for mice *IL18* Forward: ACTTTGGCCGACTTCACTGT Reverse: CAGTCTGGTCTGGGGTTCAC	Sangon Biotech	N/A
Primers for mice *S100a8* Forward: AAATCACCATGCCCTCTACAAG Reverse: CCCACTTTTATCACCATCGCAA	Sangon Biotech	N/A
Primers for mice *TNF-a* Forward: CGGGATCTCATCAGCTTCACAG Reverse: TCCTTGTTCGGAGGCAGGTCTA	Sangon Biotech	N/A
Primers for human *TNF-a* Forward: GCCCATGTTGTAGCAAACCC Reverse: TGAGGTACAGGCCCTCTGAT	Sangon Biotech	N/A
Primers for human *IL6* Forward: TCCTTCTCCACAAGCGCC Reverse: CCGTCGAGGATGTACCGAAT	Sangon Biotech	N/A
Primers for human *IL1β* Forward: CCTGAGCTCGCCAGTGAAAT Reverse: TGAAGCCCTTGCTGTAGTGG	Sangon Biotech	N/A
Primers for human *IL17A* Forward: CTGTCCCCATCCAGCAAGAG Reverse: AGGCCACATGGTGGACAATC	Sangon Biotech	N/A
Primers for human *IL18* Forward: TGGAATCAGATTACTTTGGCAAGC Reverse: GAGGCCGATTTCCTTGGTCA	Sangon Biotech	N/A

Antibodies		
β-actin	ABclonal	AC026, dilution 1: 5000
Akt	Proteintech	10176-2-AP, dilution 1: 2000
p-Akt	CellSignalingTechnology	4060, dilution 1: 2000
CCL2	ABclonal	A7277, dilution 1: 50
CD31	Abcam	ab28364, dilution 1: 50
CD68	Abcam	ab201340, dilution 1: 200
Claudin 1	Proteintech	13050-1-AP, dilution 1: 2000
CK7	Proteintech	17513-1-AP, dilution 1: 2000

F4/80	Abcam	ab6640, dilution 1: 200	
GLUT4	Proteintech	66846-1-lg, dilution 1: 2000	
iNOS	Abcam	ab178945, dilution 1: 200	
CD206	Abcam	ab64693, dilution 1: 200	
CD4	Abcam	ab133616, dilution 1: 200	
Foxp3	Abcam	ab20034, dilution 1: 200	
IRS	CellSignalingTechnology	2382, dilution 1: 2000	
p-IRS (Tyr 632)	Abcam	ab109543, dilution 1: 2000	
IκB α	CellSignalingTechnology	9242s, dilution 1: 2000	
p-IκB α	CellSignalingTechnology	9246s, dilution 1: 2000	
TLR4	Proteintech	19811-1-AP, dilution 1: 1500	
p-p65	Abcam	ab76302, dilution 1: 2000	
p65	Abcam	ab16502, dilution 1: 2000	
ZO-1	Abcam	ab190085, dilution 1: 2000	
Critical Commercial Assays			
Enhanced Chemiluminescence Assay Kit	NCM Biotech	P10300	
TNF-α ELISA	Jiangsu Meimian industrial Co. Ltd	MM-0132M1, MM-0122H1	
Insulin ELISA	Jiangsu Meimian industrial Co. Ltd	MM-0579M1	
HbA1c ELISA	Jiangsu Meimian industrial Co. Ltd	MM-1517H1, MM-0159 M2	
LPS ELISA	Cusabio and Jiangsu Meimian industrial Co. Ltd	CSB-E13066m, MM-1309H1; MM-0634M1 (for antibiotic experiment)	
DAO ELISA	Cusabio	CSB-E10090m	
Protein Assay Kit	Beyotime	P0009	
Probes used in *in situ* Hybridization			
EUB338I: GCTGCCTCCCGTAGGAG		Biossci	N/A
EUB338II: GCAGCCACCCGTAGGTGT		Biossci	N/A
EUB338III: GCTGCCACCCGTAGGTGT		Biossci	N/A
NOEUB: ACTCCTACGGGAGGCAGC		Biossci	N/A

Experimental Models: Organisms/Strains		
Mouse: C57BL6/J	Bestest	N/A
E coli	American Type Culture Collection	12014
Lachnospiraceae (K. alysoides)	American Type Culture Collection	TSD-26
Deposited data		
16S rRNA amplicon sequencing	Genome Sequence Archive	GSA: CRA012171, PRJCA018924
Software and Algorithms		
GraphPad prism 9.5.1	GraphPad Software	https://www.graphpad.com/
CaseViewer	3DHISTECH	https://www.3dhistech.com/
NDP.view 2	Hamamatsu	https://www.hamamatsu.com/
Image J	National Institutes of Health	https://imagej.net/
Image Lab	Imagelab Group	https://www.imagelab.co/

Genes or proteins acronym: *Ccl2/3*, C-C motif chemokine ligand 2/3; *Csf3*, colony stimulating factor 3; *Cxcl2*, C-X-C motif chemokine ligand 2; *Cxcl1*, C-X-C motif chemokine ligand 1; *IL1β*, interleukin 1 beta; *IL6*, interleukin 6; *IL17A*, interleukin 17A; *IL18*, interleukin 18; *S100a8*, S100 calcium binding protein A8; CD31, platelet endothelial cell adhesion molecule; CK7, cytokeratin 7; GLUT4, glucose transporter type 4; IRS, insulin receptor substrates; IκB α, IκB kinase alpha; NF-κB, nuclear factor-kappaB; TNF-α, tumor necrosis factor-α; Akt, protein kinase B; TLR-4, toll-like receptor 4; p65, RelA; ZO-1, zonula occludin 1.